Generation of an isolated sub-40-as pulse using two-color laser pulses: Combined chirp effects

Liqiang Feng[1] and Tianshu Chu[1,2,*]

[1]*State Key Laboratory of Molecular Reaction Dynamics, Dalian Institute of Chemical Physics, Chinese Academy of Sciences, Dalian, 116023, China*

[2]*Institute for Computational Sciences and Engineering, Laboratory of New Fiber Materials and Modern Textile, the Growing Base for State Key Laboratory, Qingdao University, Qingdao, 266071, China*

(Received 26 May 2011; published 28 November 2011)

In this paper, we theoretically discuss the combined chirp effects on the isolated attosecond generation when a model Ar is exposed to an intense 5-fs, 800-nm fundamental chirped pulse combined with a weak 10-fs, 1200-nm controlling chirped pulse. It shows that for the case of the chirp parameters $\beta_1 = 6.1$ (corresponding to the 800-nm field) and $\beta_2 = 4.0$ (corresponding to the 1200-nm field), both the harmonic cutoff energy and the supercontinuum can be remarkably extended resulting in a 663-eV bandwidth. Moreover, due to the introduction of the chirps, the short quantum path is selected to contribute to the harmonic spectrum. Finally, by superposing a properly selected harmonic spectrum in the supercontinuum region, an isolated pulse as short as 31 as (5 as) is generated without (with) phase compensation.

DOI: 10.1103/PhysRevA.84.053853 PACS number(s): 42.65.Ky, 42.65.Re, 42.50.Hz

I. INTRODUCTION

In the past two decades, the generation of the attosecond pulse has received much attention because of its great potential to probe the ultrafast electronic dynamics deep inside the atoms and molecules with unprecedented resolution [1–3]. Currently, several methods have been explored to generate the attosecond pulse, such as the high-order harmonic generation (HHG) from rare gases [4–7] and solid surface [8,9], relativistic nonlinear Thomson scattering (RNTS) [10,11], etc. However, the pulse intensity required in RNTS and solid surface harmonic methods is too high (higher than 10^{18} W/cm^2) to realize in a general laboratory, thus limiting their applications. On the contrary, the method of using HHG from rare gases has been successful and widely used in generating an attosecond pulse because of its requirement of moderate pulse intensity [12–14].

So far, the HHG process can be well understood by means of the well-known semiclassical three-step model [15,16], where an atom or molecule is first ionized near the peak of the intense laser field. Then, the ionized electron is accelerated away from the ion core and is drawn back to the core when the laser field reverses its direction. Finally, it can recombine with its parent ion emitting a photon with the maximum cutoff energy given by $E_{\text{cutoff}} = I_p + 3.17U_p$, where I_p is the ionization potential and U_p is the ponderomotive energy of the free electron in laser field ($U_p = e^2E^2_{\text{laser}}/4m_e\omega^2$). Further, by superposing the harmonic spectrum in the supercontinuum region, an attosecond train could be produced. But for practical application, an isolated attosecond pulse is more useful to trace the ultrafast electronic dynamics process. Currently, there are three kinds of methods that can be utilized to generate an isolated attosecond pulse. The first one is the polarization gating technology; using this technology, Sansone *et al.* experimentally obtain an isolated 130-as pulse [17]. The second one is the few-cycle driving pulse scheme, and with that an isolated 80-as pulse was experimentally realized by Goulielmakis *et al.* [18]. Very recently, the third method, namely, the two-color laser field scheme has been proposed, mainly to release the stringent requirement for the short pulse durations (shorter than 5-fs) in the above two methods. Using the two-color scheme and from the theoretical side, Zeng *et al.* [19] obtain an isolated 65-as pulse through the combination of an intense 800-nm fundamental field and a weak 400-nm controlling field. Wu *et al.* [20] obtained an isolated 38-as pulse by an intense 800-nm fundamental chirped pulse in combination with a weak 1600-nm controlling field. Xu *et al.* [21] obtained an isolated 11-as pulse through the combination of an intense 800-nm fundamental chirped pulse and a weak 800-nm controlling chirp-free pulse.

Although the chirp effects on two-color attosecond generation, such as the combination of a chirped pulse and a chirp-free subharmonic pulse [20,21], have been investigated, little study has been reported for the combination effects of the two-color chirped pulses thus far. Due to this, in this paper we theoretically discuss the combined chirp effects by investigating the HHG and isolated attosecond pulse generation when a model Ar is irradiated by an intense 5-fs, 800-nm fundamental chirped pulse combined with a weak 10-fs, 1200-nm controlling chirped pulse. The calculated results show that with the introduction of the synthesized chirp parameters ($\beta_1 = 6.1$ and $\beta_2 = 4.0$), not only the harmonic cutoff energy is remarkably extended resulting in an ultrabroad supercontinuum with a 663-eV bandwidth, but also the short quantum path is selected to contribute to the harmonic spectrum. Finally, by superposing a properly selected harmonic spectrum in the supercontinuum region, an isolated pulse as short as 31-as (5-as) is generated without (with) phase compensation.

The choice of Ar as the target atom in our calculation is due to the following considerations: First, from the practical view point, the low ionization potential energy of argon enables easier manipulation in experiments; second, from the theoretical side, the model potential used in a single-active electron picture is relatively mature for argon and can well describe its ionization structure; third, among the rather

*tschu@dicp.ac.cn; tschu008@163.com

comprehensive studies of HHG and chirp effect, there have been few studies focusing on the argon medium.

The rest of this paper is organized as follows. The computational aspects in this work are presented in Sec. II. Results and discussion are given in Sec. III. The conclusions are given in the last section. Atomic units are used throughout this paper unless stated otherwise.

II. COMPUTATIONAL ASPECTS

In our numerical calculations, the HHG and the attosecond pulse generation can be investigated by solving the time-dependent Schrödinger equation (TDSE) based on single-active electron approximation (SAE) via the parallel quantum wave-packet computer code LZH-DICP [22–28]. In the dipole approximation, the TDSE is given by

$$i\frac{\partial\phi(x,t)}{\partial t}=\left[-\frac{1}{2}\frac{\partial^2}{\partial x^2}+V(x)-xE(t)\right]\phi(x,t), \tag{1}$$

where $V(x)=-1/\sqrt{a+x^2}$ is the soft Coulomb potential with $a=1.41$ to match the ionization potential of 15.7 eV for the ground state of the Ar atom. The time-dependent wave function $\phi(x,t)$ is propagated using the standard second-order split-operator method [29–31]. The synthesized laser field is expressed as

$$E(t)=E_1 f_1(t)\cos[\omega_1 t+\delta_1(t)]+E_2 f_2(t)\cos[\omega_2 t+\delta_2(t)], \tag{2}$$

where $\delta_i(t)=-\beta_i\tanh(t/T_i)$ $(i=1,2)$ represents the carrier-envelope phases (CEPs) for the 800-nm fundamental chirp pulse and the 1200-nm controlling chirp pulse, respectively. The chirp form is controlled by the two parameters β_i and T_i $(i=1,2)$. In the present paper, we fix $T_i=200$ a.u. $(i=1,2)$. E_i and ω_i $(i=1,2)$ are the pulse intensities and the frequencies of such two chirp pulses. The envelope function is

$$f_i(t)=\exp\left[-4\ln(2)t^2/\tau_i^2\right], \tag{3}$$

where τ_i $(i=1,2)$ are the corresponding pulse durations of the two chirp pulses.

The HHG spectrum $[P_A(\omega)]$ is obtained by Fourier transforming the time-dependent dipole acceleration $a(t)$,

$$P_A(\omega)=\left|\frac{1}{\sqrt{2\pi}}\int_0^T a(t)e^{-i\omega t}dt\right|^2, \tag{4}$$

where $a(t)$ can be given by means of Ehrenfest's theorem [32],

$$a(t)=-\langle\phi(x,t)|\frac{\partial V(x)}{\partial x}-E(t)|\phi(x,t)\rangle. \tag{5}$$

Finally, the attosecond pulse can be generated by superposing several harmonics,

$$I(t)=\left|\sum_q a_q e^{i\omega t}\right|^2, \tag{6}$$

where $a_q=\int a(t)e^{-i\omega t}dt$ (inverse Fourier transformation).

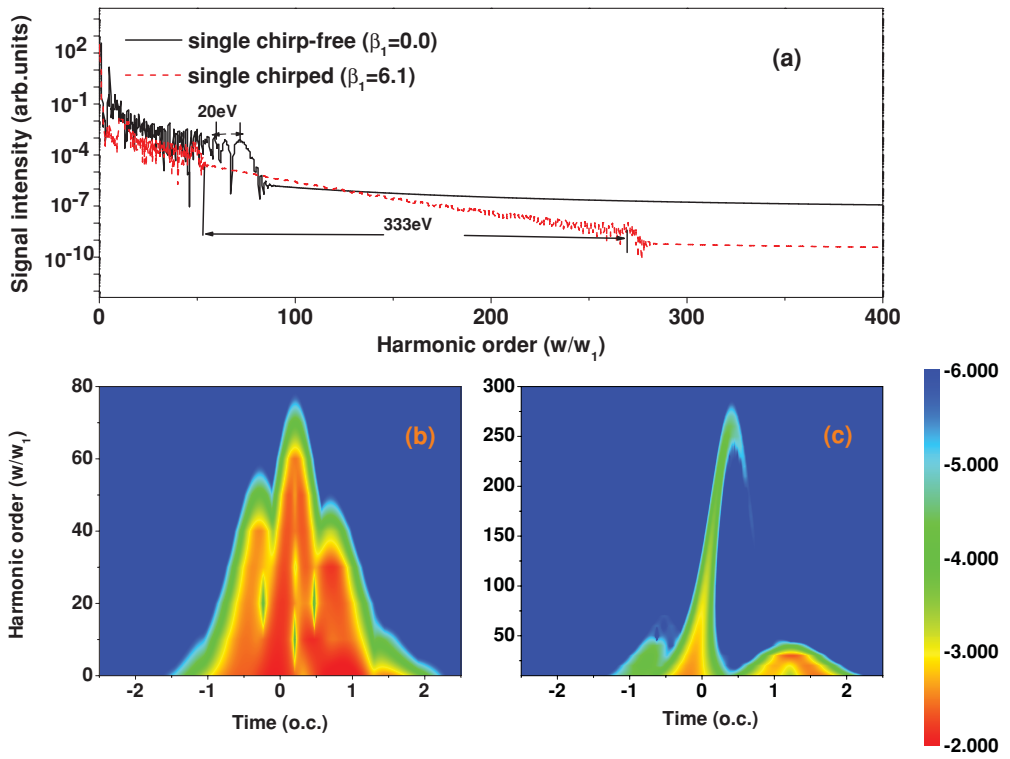

FIG. 1. (Color online) (a) HHG spectra by a single 5-fs, 800-nm $E_1=5.0\times10^{14}$ W/cm^2 fundamental chirp-free pulse ($\beta_1=0.0$, solid black line) and a single-fundamental chirped pulse ($\beta_1=6.1$, dashed red line). (b) and (c) The corresponding time-frequency distributions for the fundamental chirp-free pulse and chirped pulse, respectively. Here, o. c. denotes the optical cycle of the 800-nm laser field.

III. RESULTS AND DISCUSSION

Figure 1(a) depicts the HHG spectra from Ar driven by the single 5-fs, 800-nm fundamental chirp-free pulse ($\beta_1 = 0$) and the single chirped pulse ($\beta_1 = 6.1$; this is what we find for the optimal value for Ar under the present laser field). The pulse intensity of the fundamental field is chosen to be $E_1 = 5.0 \times 10^{14}$ W/cm^2. For the chirp-free pulse case (solid black line), the maximum cutoff energy is the 71st-order harmonic (corresponding to 110 eV) which is in quantitative agreement with the classical prediction $E_{\text{maximum}} = I_p + 3.17U_p$. With the introduction of the chirp (dashed red line), the maximum cutoff energy is remarkably extended, resulting in an ultrabroad supercontinuum (i.e., the region between the maximum cutoff energy and the second maximum cutoff energy) with a 333-eV bandwidth. Moreover, the interference structure [33] between the two quantum paths, namely, the long quantum path (earlier ionization, later recollision) and the short quantum path (later ionization, earlier recollision), is smaller than that of the chirp-free pulse. It is well known that each emitted harmonic receives these two quantum path contributions and the less modulated supercontinuum contributed by the single quantum path is more beneficial to generate the isolated attosecond pulse [34,35]. In order to analyze such two quantum path contributions, in Figs. 1(b) and 1(c), we present the time-frequency distributions of HHG for the above two cases by using the wavelet transformation of the dipole acceleration $a(t)$ [36,37],

$$A(t,\omega) = \int a(t')\sqrt{\omega}W\left[\omega(t'-t)\right]dt', \tag{7}$$

where $W[\omega(t'-t)]$ is the mother wavelet. In general, the natural choice of the mother wavelet is a Morlet wavelet [38],

$$W(x) = \left(\frac{1}{\sqrt{\alpha}}\right)e^{ix}e^{-x^2/2\tau^2}, \tag{8}$$

where $\alpha = 30$ in our calculations. It shows that for the chirped pulse case [Fig. 1(c)], the contribution of the short quantum path is much more intense than that of the long quantum path for the supercontinuum region, which is responsible for the little modulation on the HHG spectrum, while for the chirp-free pulse case [Fig. 1(b)], there are similar intensity contributions from both quantum paths causing more obvious interference structure.

Further understanding of the harmonic spectral characteristics and the harmonic cutoff energy extension with the chirped pulse can be gained through Fig. 2, where the dependence of the kinetic energies on the ionization and recombination times are presented for the above two cases, respectively. Clearly, there are three main peaks on the ionization and recombination energy map for the chirp-free case [Fig. 2(b)], which should be caused by three occurrences of the "three-step process" [23,39], marked as A-B-C (ionization-acceleration-recombination), B-C-D, and C-D-E in the profile of the laser field in Fig. 2(a) (denoted by the solid black line). The maximum peak value is the 71st-order harmonic, in excellent agreement with the quantum result shown in Fig. 1(a). In the

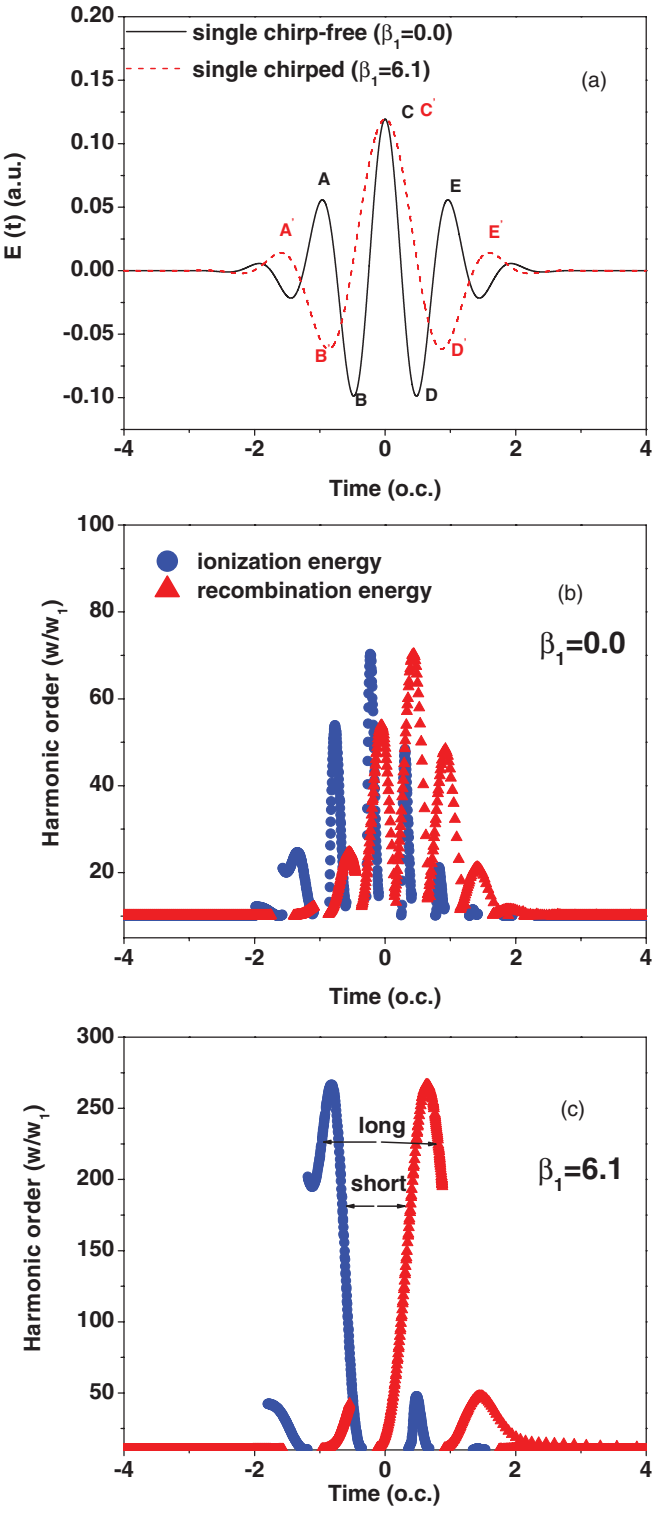

FIG. 2. (Color online) (a) The profiles of the laser fields for the single-fundamental chirp-free pulse (solid black line) and chirped pulse (dashed red line). (b) and (c) The ionizing and returning energy maps for the single-fundamental chirp-free pulse and chirped pulse, respectively.

case of the chirped pulse [Fig. 2(c)], there are also three main peaks, but the maximum peak determined by the B′-C′-D′ process has been obviously enhanced. Turning to the profile of the chirped laser field shown in Fig. 2(a) (dashed red line),

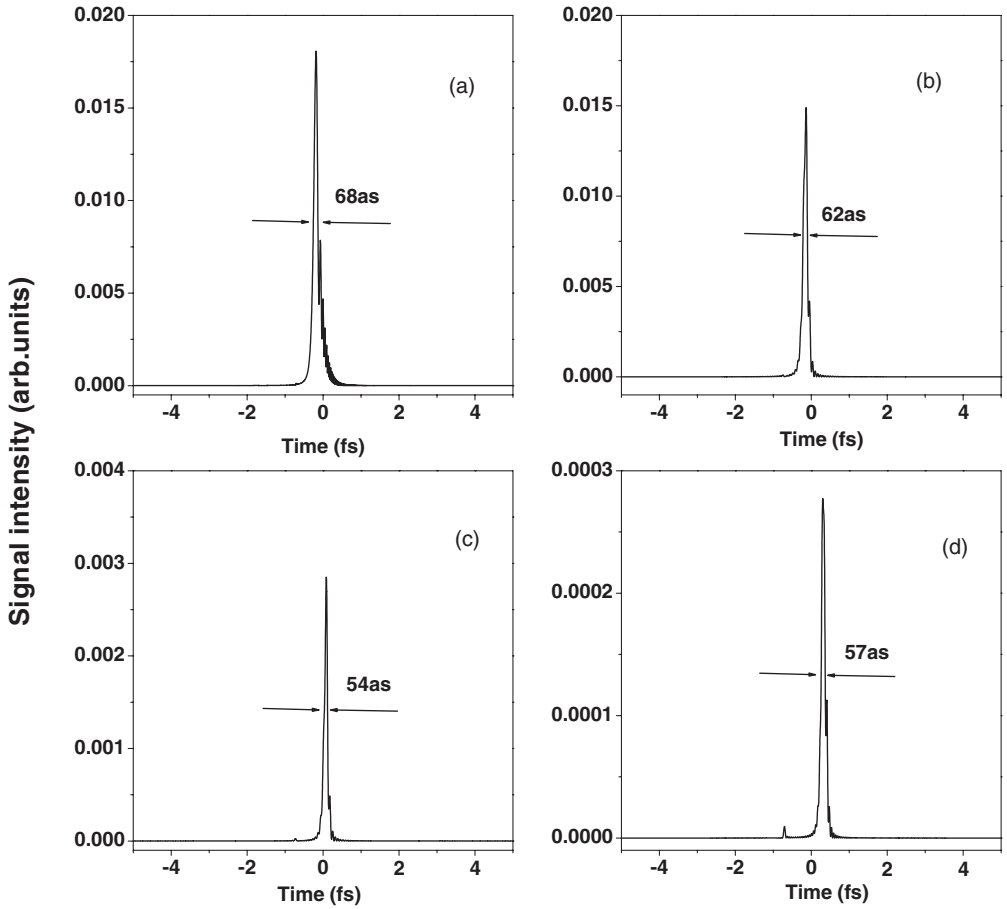

FIG. 3. The temporal profiles of the attosecond pulses by superposing several orders of the harmonics: (a) the total supercontinuum region, (b) from the 60th to the 100th order, (c) from the 100th to the 160th order, (d) from the 160th to the 215th order, for the single-fundamental chirped pulse case.

we can see that with the introduction of the chirp, albeit the intensity of the amplitude (peak C or C′) remains unchanged but the B′-C′-D′ process has been obviously broadened; therefore, the electron must take much more time in its processes of accelerating and returning to the parent ion, which is responsible for the extension of the cutoff energy [21,40,41]. Moreover, as seen in Fig. 2(c), the short quantum path can be easily selected to contribute to the higher-order harmonics that is beneficial to generate the isolated attosecond pulse, just as that shown in the time-frequency analysis in Fig. 1(c).

Figure 3 shows the temporal profiles of the generated isolated attosecond pulses by superposing the different-order harmonics for the single chirped pulse case. First, in Fig. 3(a), by superposing the total supercontinuum region from the 57th to the 272nd order, a 68-as pulse with accompanying satellite pulses can be obtained. Due to the fact that the harmonics do not emit at the same time, the selection of an entire supercontinuum region no longer provides the perfect possible situation for generating an attosecond pulse. By properly superposing the harmonics from the 60th to the 100th order, from the 100th to the 160th order, or from the 160th to the 215th order, the satellite pulses have been suppressed, and an isolated pulse of 62, 54, or 57-as has been respectively obtained, as shown in Figs. 3(b)–3(d). In addition, there is a small pulse showing up before the main 57-as pulse in Fig. 3(d), which should be attributed to the long quantum path (this situation can also be found in Figs. 3(a)–3(c), but due to the intensity being even less, the small pulse can be negligible). This is further supported by the fact that such a small pulse will be enhanced when we continue to superpose the harmonics higher than the 220th order, since the long quantum path again began to make its contribution for the harmonic higher than the 220th order, as vividly shown in Fig. 1(c).

Thus, the use of the single-fundamental chirped pulse can obtain an isolated sub-100-as attosecond pulse, but it is still longer than 50-as. To obtain even shorter attosecond pulses, we proposed a scheme of utilizing the combined chirp effects by adding a controlling chirped pulse to the fundamental chirped ($\beta_1 = 6.1$) pulse. The idea is enlightened by the fact that adding a subharmonic pulse onto the fundamental chirped pulse will keep extending the cutoff energy and thus reduce the pulse duration of the attosecond pulse [20,21].

Figure 4(a) depicts the HHG spectra under the synthesized laser field by adding a second controlling pulse where the chirp parameter β_2 is chosen to be $\beta_2 = 0.0$ (chirp-free, solid black line), 1.0 (dashed red line) and 4.0 (dash-dot blue

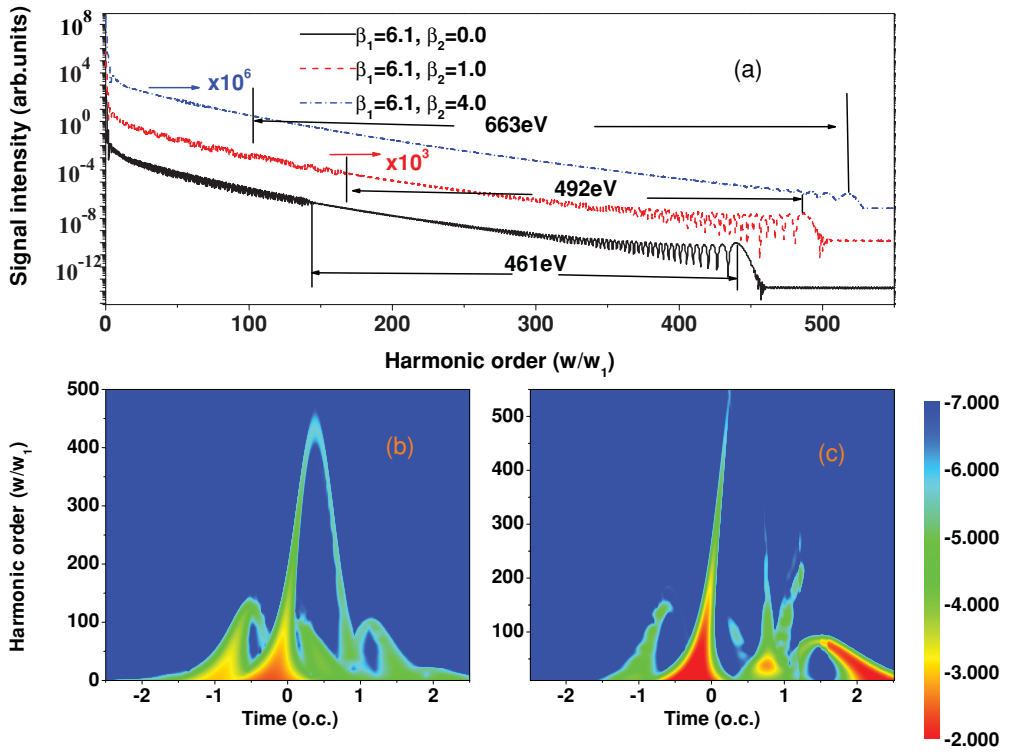

FIG. 4. (Color online) (a) HHG spectra by the fundamental chirped pulse combined with a 10-fs, 1200-nm, $E_2 = 1.0 \times 10^{14}$ W/cm^2 controlling chirp-free pulse ($\beta_2 = 0.0$, solid black line) or a chirped pulse ($\beta_2 = 1.0$, dashed red line, $\beta_2 = 4.0$, dash-dot blue line). (b) and (c) The corresponding time-frequency distributions for adding the chirp-free pulse ($\beta_2 = 0.0$) and the chirped pulse ($\beta_2 = 4.0$), respectively.

line; this is what we find for the optimal value for Ar atom under the present synthesized field). The other parameters of the controlling chirp pulse are 10-fs, 1200-nm, $E_2 = 1.0 \times 10^{14}$ W/cm^2. Clearly, we see that with the introduction of the controlling chirp-free pulse, the harmonic cutoff energy and the supercontinuum are all enhanced. And with the increasing of the chirp parameter β_2, not only the harmonic cutoff energy keeps enhancing, but also the interference structure between the two quantum paths is being suppressed. Especially for $\beta_2 = 4.0$, there is an optimum condition covering a 663-eV supercontinuum bandwidth. To analyze the two quantum path contributions to the HHG spectra, in Figs. 4(b) and 4(c), we present the time-frequency distributions of the HHG spectra for the cases of $\beta_2 = 0.0$ and 4.0 ($\beta_1 = 6.1$), respectively. Clearly, for the $\beta_2 = 0.0$ case [Fig. 4(b)], the contributions of the two quantum paths in the supercontinuum region from the 240th to the 440th order are almost the same, which is responsible for the obvious interference structure on the HHG spectrum. While for the case of $\beta_2 = 4.0$ [Fig. 4(c)], the contribution of the long quantum path is largely suppressed, leading to the short quantum path being finally selected to contribute to the HHG spectrum from the 150th to the 518th order, which supports generation of a favorable isolated attosecond pulse.

The corresponding dependence of the kinetic energies on the ionization and recombination times for the combined chirp case ($\beta_1 = 6.1$ and $\beta_2 = 4.0$) is shown in Fig. 5(b), further providing insights into the physical origin of the harmonic cutoff energy extension by adding the controlling chirped pulse. The ionization and recombination energies map demonstrates three main peaks caused by three occurrences of the recollision processes as we discussed before. That the maximum peak is extended to the 518th-order harmonic agrees well with the quantum result shown in Fig. 4(a). From the profile of the laser field in Fig. 5(a), we see that not only the amplitude of peak C is enhanced but also the process B-C-D is a little broadened with the introduction of the controlling chirped pulse ($\beta_2 = 4.0$). As a consequence, the electron gained much more energy and spent a little more time in accelerating and returning processes, which is responsible for the extension of the cutoff energy.

The two previous studies [21,42] showed that increasing the pulse intensity of the controlling laser field will keep enhancing the bandwidth of the supercontinuum region. However, this does not work in the present case using the combined chirp effects. The HHG spectra we calculated for the cases of $E_2 = 3.0 \times 10^{14}$ W/cm^2 (solid black line) and 5.0×10^{14} W/cm^2 (dashed red line) in Fig. 6 have illustrated that the supercontinuum region on the HHG spectrum is deteriorated at higher controlling pulse intensity. Thus, our original choice of $E_2 = 1.0 \times 10^{14}$ W/cm^2 has already been the limitation for the controlling chirped pulse.

Figure 7 shows the temporal profiles of the generated isolated attosecond pulses for the optimal synthesized two-color chirped pulse. First, by superposing the harmonics from the 90th to the 518th order (the total supercontinuum region), a 46-as pulse with some satellite pulses has been obtained, as shown in Fig. 7(a). In order to obtain an isolated

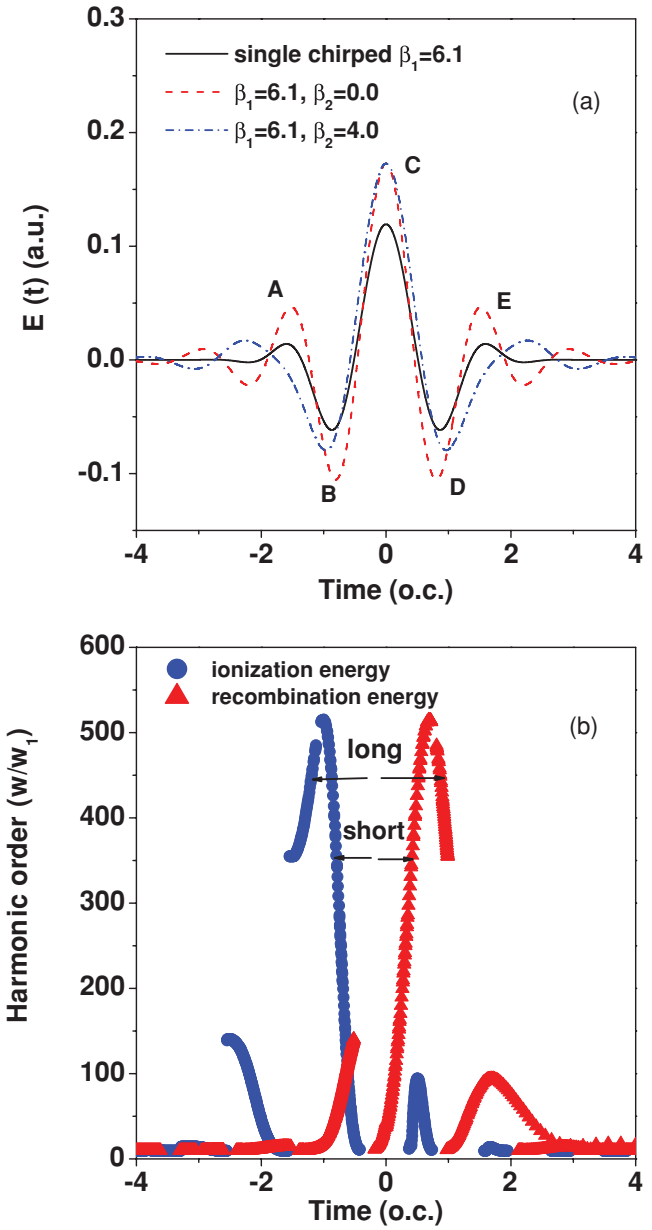

FIG. 5. (Color online) (a) The profiles of the laser fields for the single-fundamental chirped pulse ($\beta_1 = 6.1$, solid black line), the fundamental chirped pulse combined with the controlling chirp-free pulse ($\beta_1 = 6.1$, $\beta_2 = 0.0$, dashed red line), and the fundamental chirped pulse combined with the controlling chirped pulse ($\beta_1 = 6.1$, $\beta_2 = 4.0$, dash-dot blue line). (b) The corresponding ionizing and returning energy maps for the fundamental chirped pulse combined with the controlling chirped pulse ($\beta_1 = 6.1$, $\beta_2 = 4.0$).

attosecond pulse with high signal-to-noise ratio, next, we will only superpose a section of the harmonics from the supercontinuum region. As shown in Figs. 7(b) and 7(c), by properly superposing the harmonics from the 100th to the 150th order or from the 150th to the 210th order, an isolated attosecond pulse with duration of 40 or 31-as has been obtained without any phase compensation. It should be noted that the pulse intensity of the 31-as pulse is one order of magnitude lower than that of the 40-as pulse. If we superpose the harmonics higher than the 210th order,

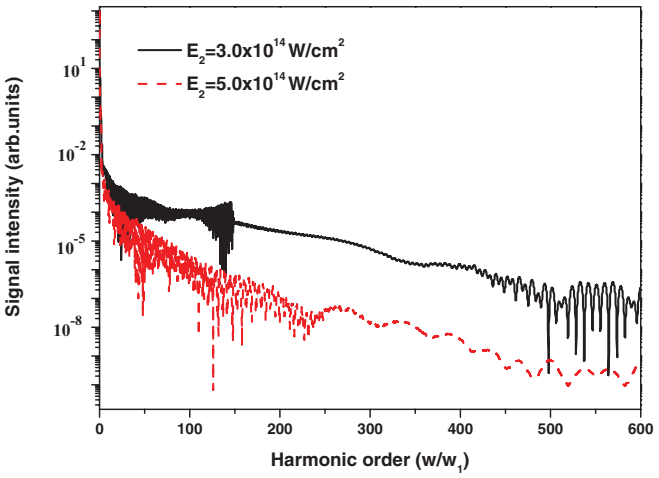

FIG. 6. (Color online) HHG spectra by the fundamental chirped pulse combined with the controlling chirped pulse ($\beta_1 = 6.1$, $\beta_2 = 4.0$) at pulse intensity $E_2 = 3.0 \times 10^{14}$ W/cm^2 (solid black line) and $E_2 = 5.0 \times 10^{14}$ W/cm^2 (dashed red line).

there is no further improvement in the pulse duration of the generating attosecond pulse (no longer shorter than 31-as) but the pulse intensity is found to be remarkably decreased. Finally, with the proper compensation for the phase dispersion, an impressive isolated 5-as pulse can be achieved, as shown in Fig. 7(d).

Thus we showed here that the combined chirp effects with the same chirp form of $\delta(t) = -\beta\tanh(t/T)$ is favorable for the experimental realization of the ultrashort single pulse generation and with argon gas. More specifically, for an argon atom irradiated by the 5-fs, 800-nm + 10-fs,1600-nm laser pulses, the two chirp parameters of $\beta_1 = 6.1$ and $\beta_2 = 4.0$, as well as the moderate pulse intensities of $\sim 10^{14}$ W/cm^2 are the most favorable conditions. As a consequence, the moderate pulse intensities in our proposed scheme are easier to obtain as compared with the former studies ($\sim 10^{15}$ W/cm^2) [20,21], and the same chirp form of the two-color field is also beneficial to experimental realization. The present generated ultrashort 5-as pulse with phase compensation may open a new way to the zeptosecond (zs) scale [43], but the phase compensation technique still poses an experimental challenge. On the other side, the present isolated 31-as pulse without phase compensation is short enough to probe the ultrafast electronic dynamics deep inside the atoms or molecules.

IV. CONCLUSION

In conclusion, we have theoretically investigated the combined chirp effects on generations of HHG and attosecond pulse with a two-color chirped pulse. Our results show that with the introduction of the chirps ($\beta_1 = 6.1$ and $\beta_2 = 4.0$) the harmonic cutoff energy is remarkably extended resulting in an ultrabroad supercontinuum with a 663-eV bandwidth, as compared with the cases of the single-fundamental chirp-free pulse, the single-fundamental chirped pulse, and the fundamental chirped pulse combined with the controlling chirp-free pulse. Moreover, due to the combined chirp effects,

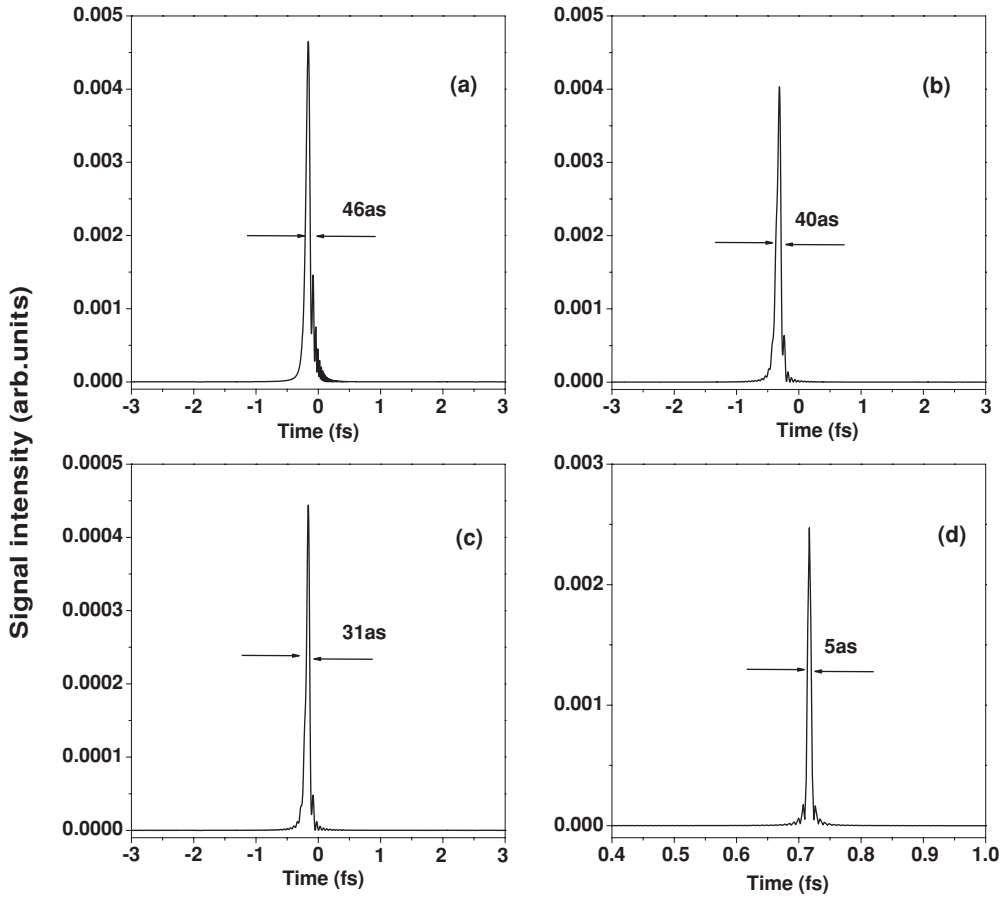

FIG. 7. The temporal profiles of the attosecond pulses in the synthesized two-color chirped pulse ($\beta_1 = 6.1$, $\beta_2 = 4.0$), where the pulse intensity is $E_2 = 1.0 \times 10^{14}$ W/cm^2. (a) Attosecond pulse by superposing harmonics from the 90th to the 518th order (the total supercontinuum region). (b) and (c) Attosecond pulses by superposing harmonics from the 100th to the 150th order and from the 150th to the 210th order. (d) Attosecond pulses by superposing the total supercontinuum region with phase compensation.

the supercontinuum region of the HHG spectrum is nearly contributed by the short quantum path which is beneficial in generating the isolated attosecond pulse. As a consequence, by superposing some properly selected harmonics, an isolated 31-as (5-as) pulse with high signal-to-noise ratio is obtained without (with) phase compensation.

ACKNOWLEDGMENTS

The authors thank Professor Keli Han for providing us the computational code used in the present work. This work is supported by NSFC (Grants No. 10874096 and No. 20633070).

[1] M. Uiberacker *et al.*, Nature **446**, 627 (2007).
[2] S. Haessler *et al.*, Nat. Phys. **6**, 200 (2010).
[3] G. Sansone *et al.*, Nature **465**, 763 (2010).
[4] F. Krausz, Rev. Mod. Phys. **81**, 163 (2009).
[5] I. Osborne and J. Yeston, Science **317**, 765 (2007).
[6] P. Agostini and L. DiMauro, Rep. Prog. Phys. **67**, 813 (2004).
[7] K. Ishikawa, Phys. Rev. Lett. **91**, 043002 (2003).
[8] G. D. Tsakiris, K. Eidmann, J. Meyer-ter-Vehn, and F. Krausz, New J. Phys. **9**, 019 (2006).
[9] B. Dromey *et al.*, Phys. Rev. Lett. **99**, 085001 (2007).
[10] J. Gao, Phys. Rev. Lett. **93**, 243001 (2004).
[11] K. Lee, Y. H. Cha, M. S. Shin, B. H. Kim, and D. Kim, Opt. Express **11**, 309 (2003).
[12] B. Kim, J. Ahn, Y. L. Yu, Y. Cheng, Z. Z Xu, and D. E. Kim, Opt. Express **16**, 10331 (2008).
[13] Z. Zhai, R. F. Yu, X. S. Liu, and Y. J. Yang, Phys. Rev. A **78**, 041402 (2008).
[14] P. Zou, Z. N. Zeng, Y. H. Zheng, Y. Y. Lu, P. Liu, R. X. Li, and Z. Z. Xu, Phys. Rev. A **81**, 033428 (2010).
[15] P. B. Corkum, Phys. Rev. Lett. **71**, 1994 (1993).
[16] J. L. Krause, K. J. Schafer, and K. C. Kulander, Phys. Rev. Lett. **68**, 3535 (1992).
[17] G. Sansone *et al.*, Science **314**, 443 (2006).
[18] E. Goulielmakis *et al.*, Science **320**, 1614 (2008).
[19] Z. Zeng, Y. Cheng, X. Song, R. Li, and Z. Xu, Phys. Rev. Lett. **98**, 203901 (2007).
[20] J. Wu, G. T. Zhang, C. L. Xia, and X. S. Liu, Phys. Rev. A **82**, 013411 (2010).
[21] J. J. Xu, B. Zeng, and Y. L. Yu, Phys. Rev. A **82**, 053822 (2010).

[22] R. F. Lu, P. Y. Zhang, and K. L. Han, Phys. Rev. E **77**, 066701 (2008).
[23] R. F. Lu, H. X. He, Y. H. Guo, and K. L. Han, J. Phys. B: At. Mol. Opt. Phys. **42**, 225601 (2009).
[24] J. Hu, K. L. Han, and G. Z. He, Phys. Rev. Lett. **95**, 123001 (2005).
[25] J. Hu, M. S. Wang, K. L. Han, and G. Z. He, Phys. Rev. A **74**, 063417 (2006).
[26] J. Hu, Q. T. Meng, and K. L. Han, Chem. Phys. Lett. **442**, 17 (2007).
[27] H. Zhang *et al.*, Chem. Phys. Lett. **271**, 204 (1997).
[28] H. Zhang *et al.*, Chem. Phys. Lett. **289**, 494 (1998).
[29] T. S. Chu, Y. Zhang, and K. L. Han, Int. Rev. Phys. Chem. **25**, 201 (2006).
[30] K. L. Han and G. Z. He, J. Photochem. Photobiol. C **8**, 55 (2007).
[31] T. S. Chu and K. L. Han, Phys. Chem. Chem. Phys. **10**, 2431 (2008).
[32] K. Burnett, V. C. Reed, J. Cooper, and P. L. Knight, Phys. Rev. A **45**, 3347 (1992).
[33] Y. Mairesse *et al.*, Science **302**, 1540 (2003).
[34] W. Hong, P. Lu, W. Cao, P. Lan, and X. Wang, J. Phys. B: At. Mol. Opt. Phys. **40**, 2321 (2007).
[35] J. G. Chen, Y. J. Yang, S. L. Zeng, and H. Q. Liang, Phys. Rev. A **83**, 023401 (2011).
[36] J. J. Carrera and Shih-I Chu, Phys. Rev. A **75**, 033807 (2007).
[37] J. J. Carrera, X. M. Tong, and Shih-I Chu, Phys. Rev. A **74**, 023404 (2006).
[38] P. Antoine, B. Piraux, and A. Maquet, Phys. Rev. A **51**, R1750 (1995).
[39] Y. H. Guo, R. F. Lu, K. L. Han, and G. Z. He, Int. J. Quant. Chem. **109**, 3410 (2009).
[40] J. Wu, Z. Zhai, and X. S. Liu, Chin. Phys. B **19**, 093201 (2010).
[41] L. Q. Feng and T. S. Chu, Phys. Lett. A **375**, 3641 (2011).
[42] T. J. Shao, G. J. Zhao, B. Wen, and H. Yang, Phys. Rev. A **82**, 063838 (2010).
[43] M. C. Kohler, C. H. Keitel, and K. Z. Hatsagortsyan, Opt. Express **19**, 4411 (2011).